Insights into carbonation kinetics of fly ash from Victorian lignite for CO_2 sequestration

Long Ji[a, b, c], Hai Yu[b*], Bing Yu[b], Ruijie Zhang[c], David French[d], Mihaela Grigore[e], Xiaolong Wang[f], Zuliang Chen[g], Shuaifei Zhao[a**]

[a] Department of Environmental Sciences, Macquarie University, Sydney, NSW 2109, Australia

[b] CSIRO Energy, Newcastle, NSW 2304, Australia

[c] China University of Mining & Technology Beijing, Beijing, 100083, China

[d] University of New South Wales, Sydney, NSW 2052, Australia

[e] CSIRO Energy, North Ryde, NSW 2113, Australia

[f] Huaneng Clean Energy Research Institute, Beijing, 102209, China

[g] Fujian Key Laboratory of Pollution Control and Resource Reuse, School of Environmental Science and Engineering, Fujian Normal University, Fuzhou 350007, China

*Corresponding author Ph: +61-2-4960-6201 Email: hai.yu@csiro.au

**Corresponding author Ph: +61 2 9850-9672 Email: shuaifei.zhao@mq.edu.au;

Supporting information

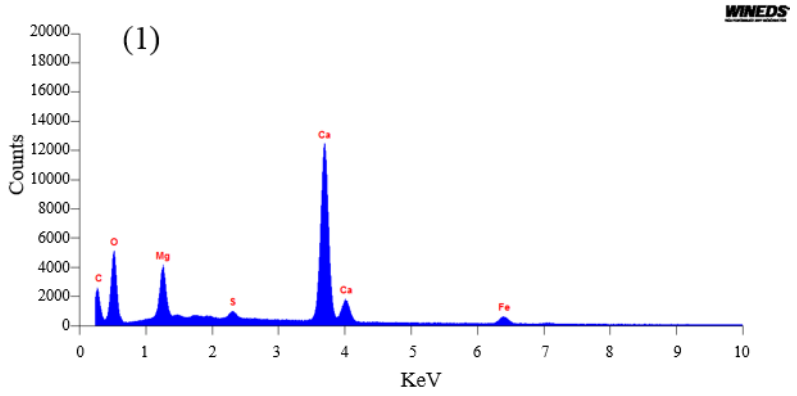
WINEDS
(1)
Counts
KeV
C
O
Mg
S
Ca
Ca
Fe

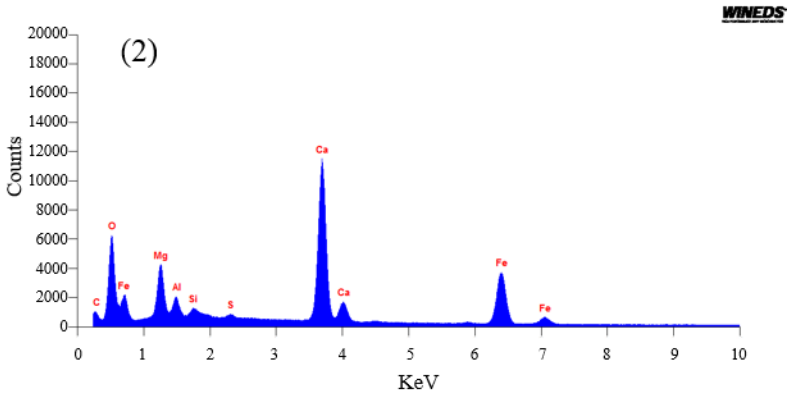
WINEDS
(2)
Counts
KeV
C
O
Fe
Mg
Al
Si
S
Ca
Ca
Fe
Fe

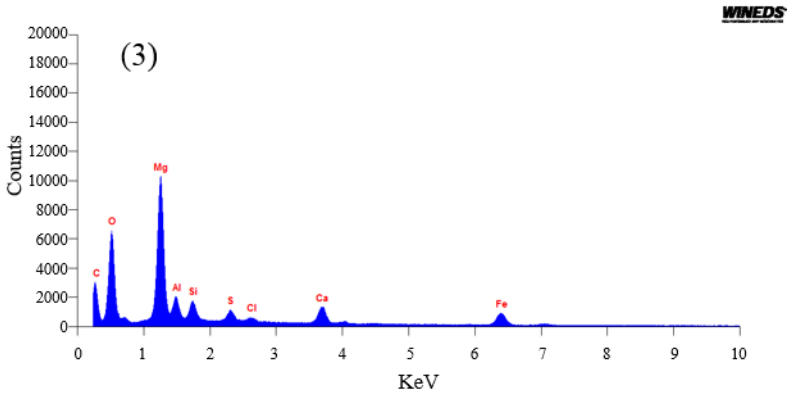
WINEDS
(3)
Counts
KeV
C
O
Mg
Al
Si
S
Cl
Ca
Fe

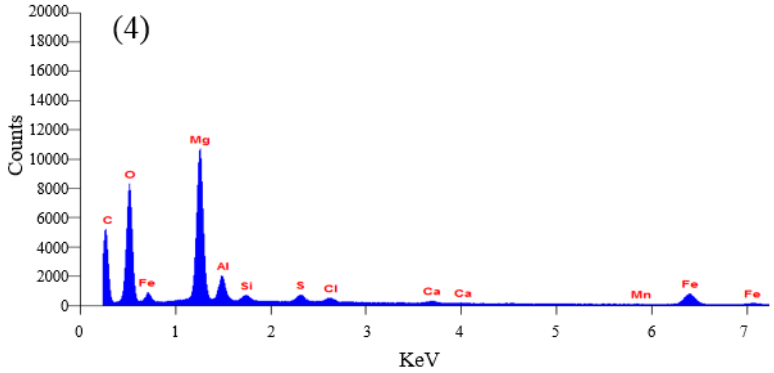
(4)
Counts
KeV
C
O
Fe
Mg
Al
Si
S
Cl
Ca
Ca
Mn
Fe
Fe

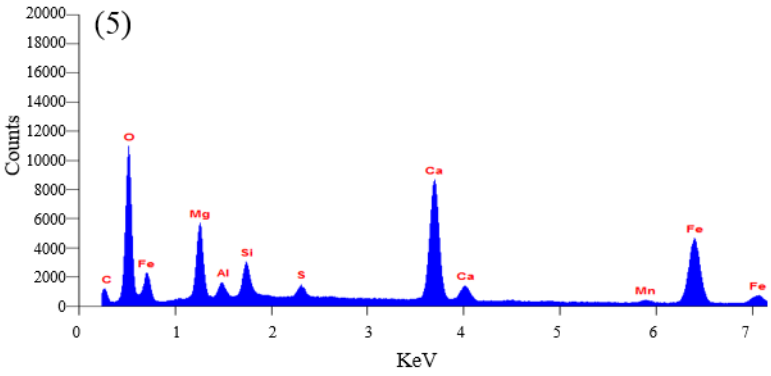
(5)
Counts
KeV
C
O
Fe
Mg
Al
Si
S
Ca
Ca
Mn
Fe
Fe

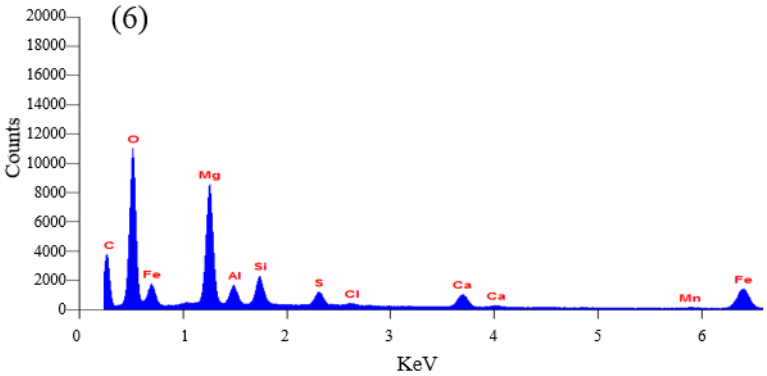
(6)
Counts
KeV
C
O
Fe
Mg
Al
Si
S
Cl
Ca
Ca
Mn
Fe

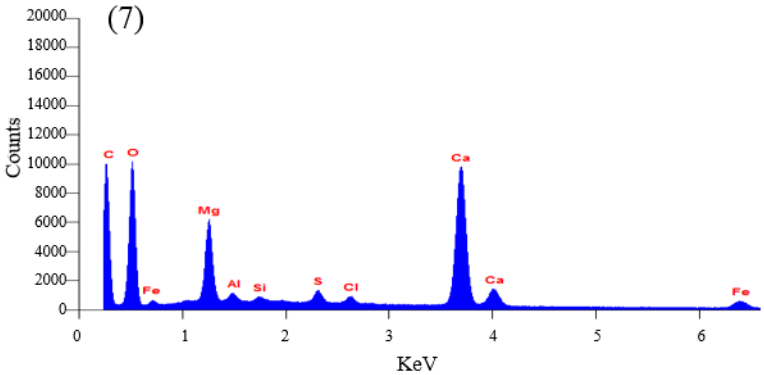
(7)
Counts
KeV
C
O
Fe
Mg
Al
Si
S
Cl
Ca
Ca
Fe

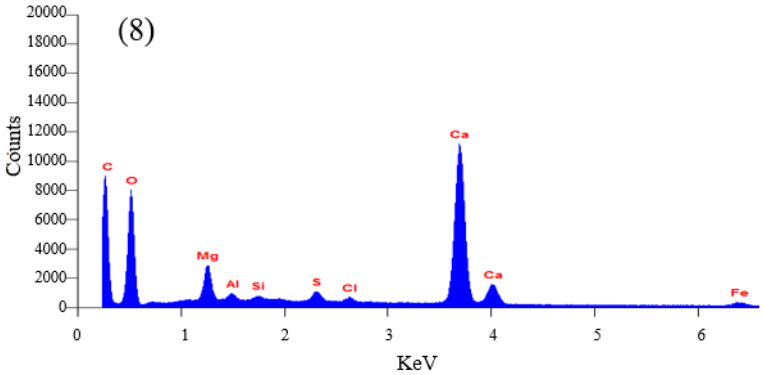
(8)
Counts
KeV
C
O
Mg
Al
Si
S
Cl
Ca
Ca
Fe

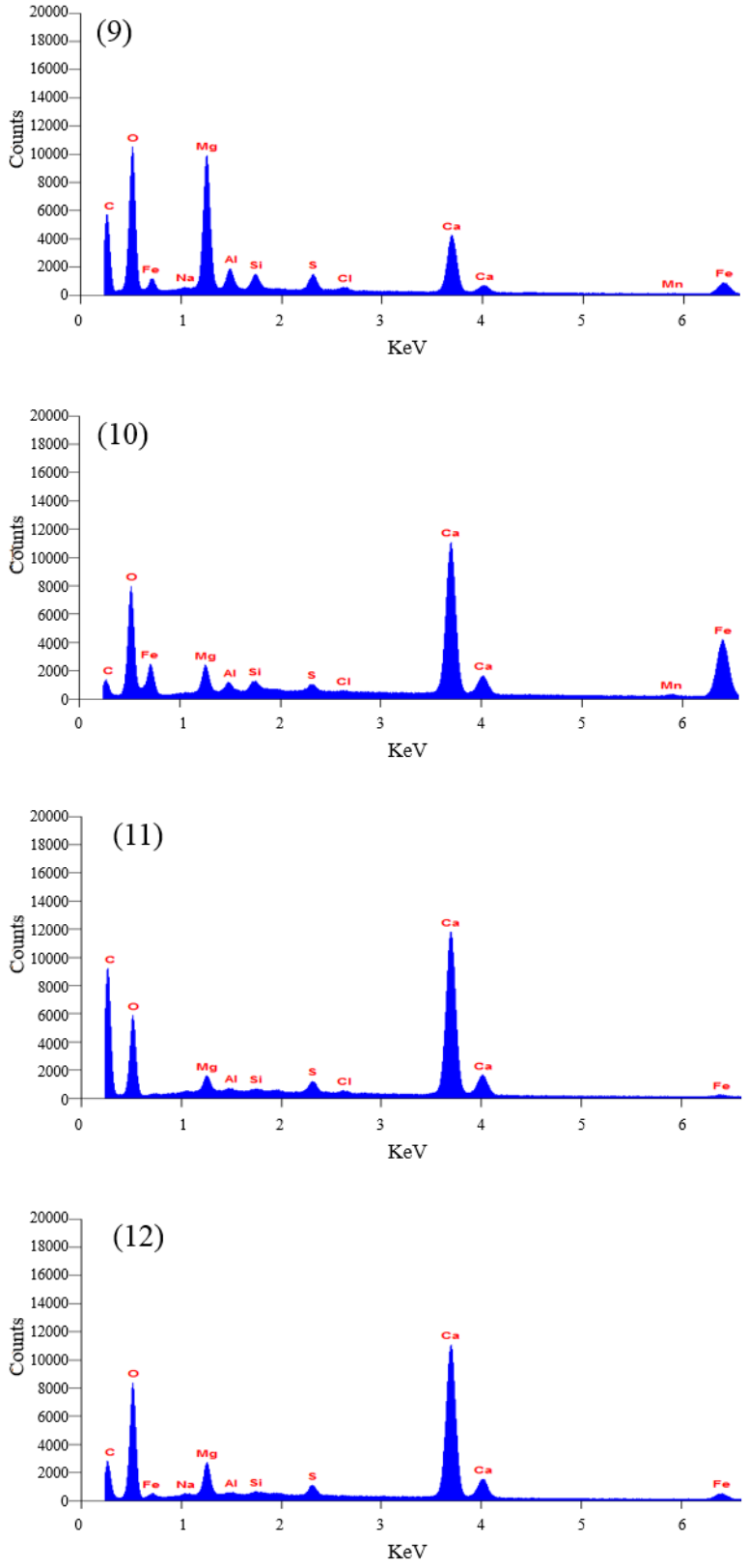

Figure S1 EDS patterns for the spots of carbonated sample in Figure 5

Figure S1 shows the EDS patterns of the 12 spots of the carbonated sample in Figure 5 (temperature, 40ºC; stirring rate, 900 rpm; CO_2 pressure, 4bar). With the semi-quantitative chemical analysis provided by EDS, it is possible to identify the elemental composition of the precipitates and the unreacted ash particles.

List of figures

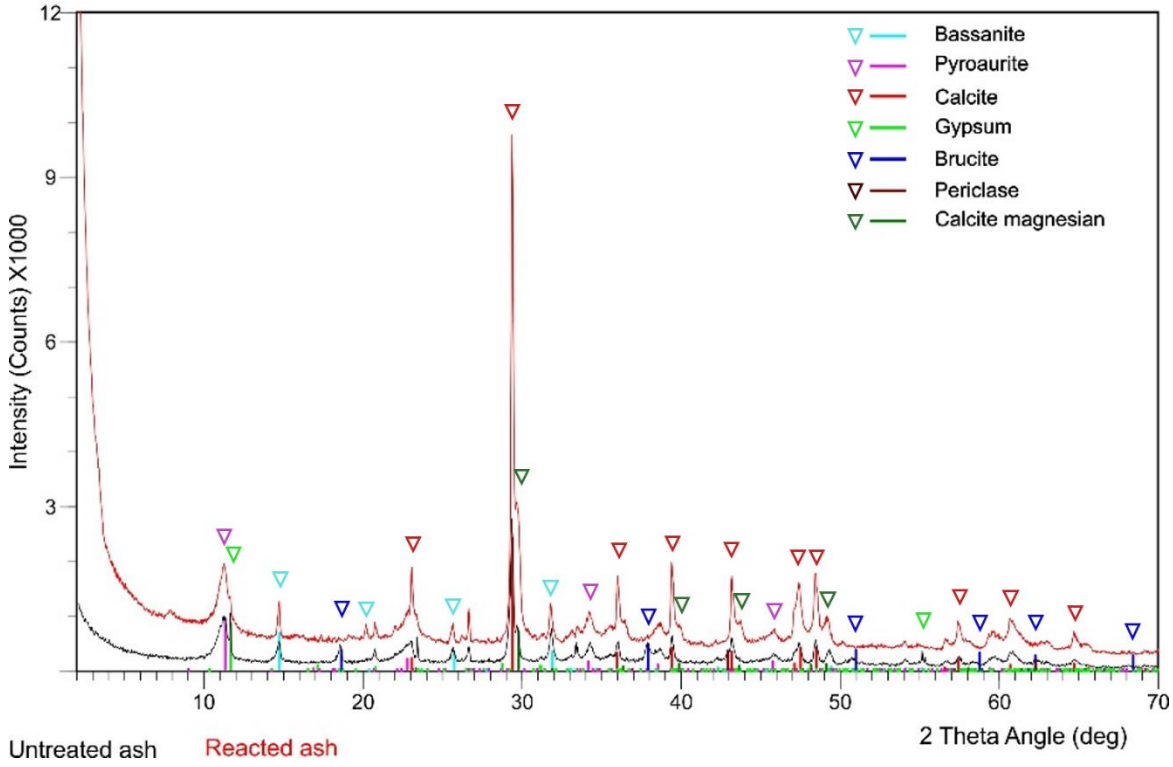

Figure 1: X-ray diffraction patterns of fresh and carbonated ash

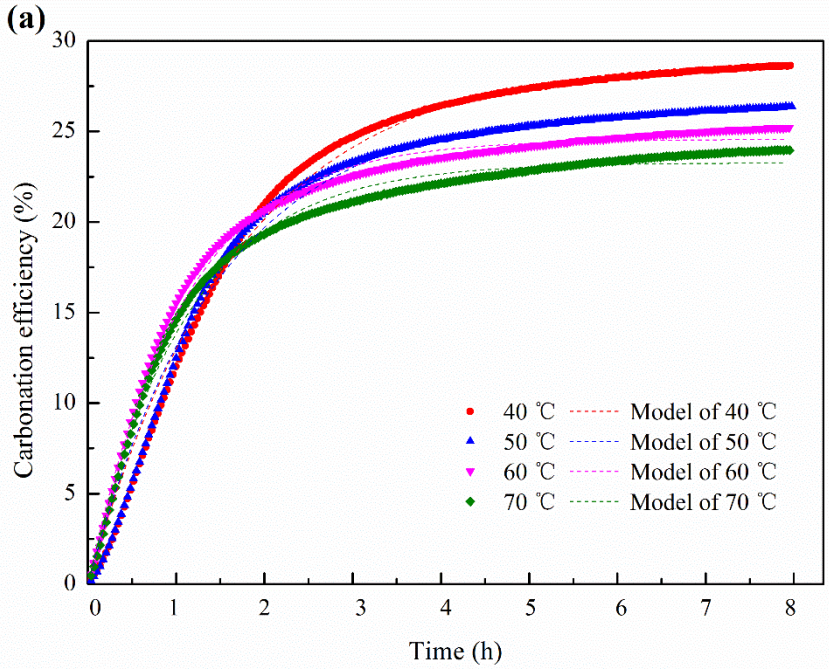
(a)
Carbonation efficiency (%)
Time (h)
40 ℃
50 ℃
60 ℃
70 ℃
Model of 40 ℃
Model of 50 ℃
Model of 60 ℃
Model of 70 ℃

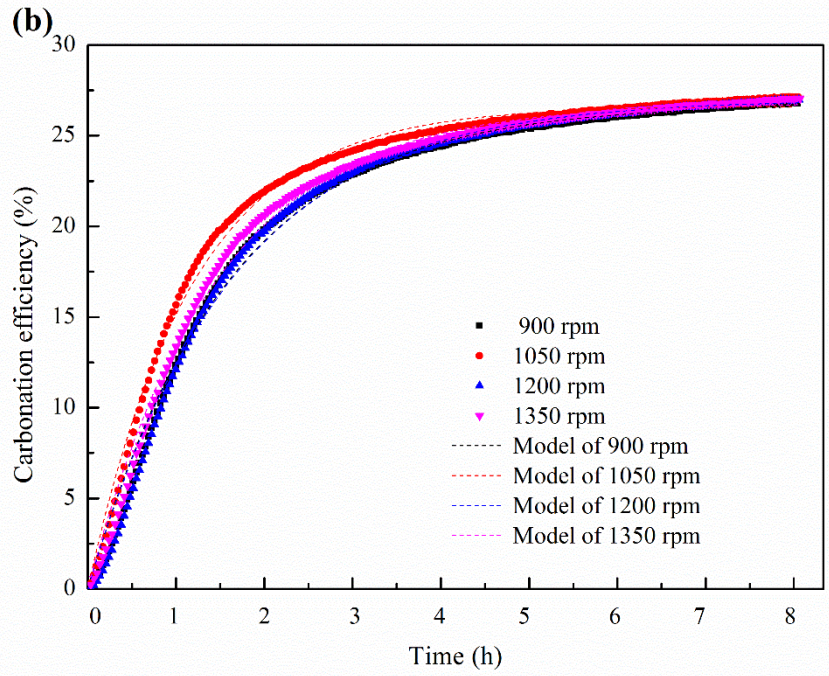
(b)
Carbonation efficiency (%)
Time (h)
900 rpm
1050 rpm
1200 rpm
1350 rpm
Model of 900 rpm
Model of 1050 rpm
Model of 1200 rpm
Model of 1350 rpm

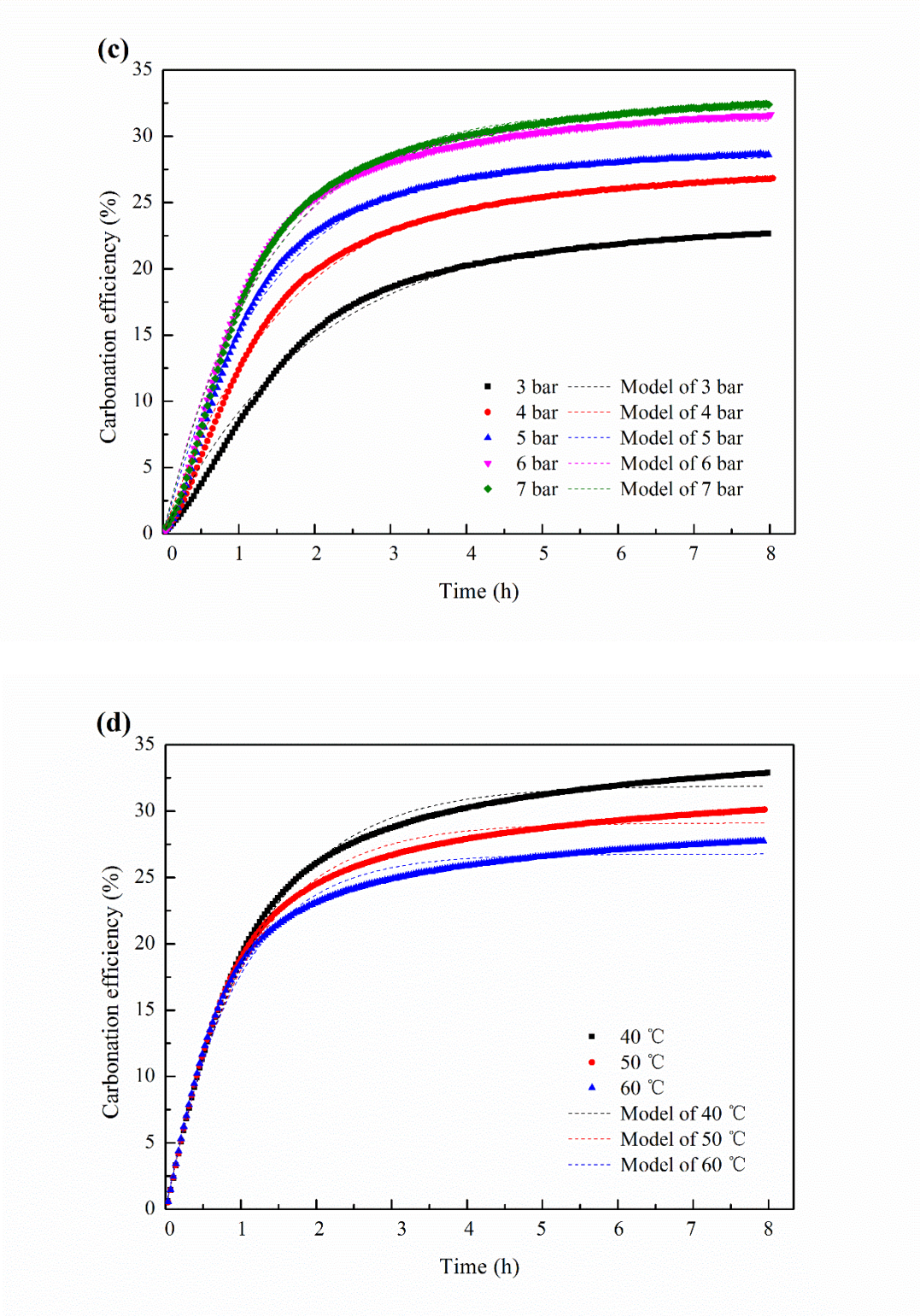

Figure 2 Model fitting results of carbonation experiments at (a) various temperatures (30, 40, 50, 60 and 70 °C) (stirring rate, 900 rpm; CO_2 pressure, 4 bar); (b) various stirring rates (900, 1050, 1200 and 1350 rpm) (temperature, 40 °C; CO_2 pressure, 4 bar); (c) various CO_2 pressures (3, 4, 5, 6 and 7

bar) (temperature, 40 °C; stirring rate, 900 rpm); and (d) various temperatures (40, 50 and 60 °C) (stirring rate, 900 rpm; CO_2 pressure, 4 bar; additive, 0.5 mol/L $NaHCO_3$)

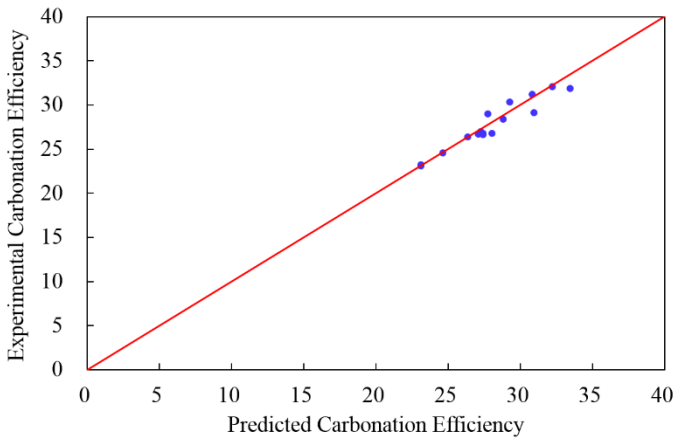

Figure 3 Comparison of the predicted carbonation efficiency of fly ash by the surface coverage model

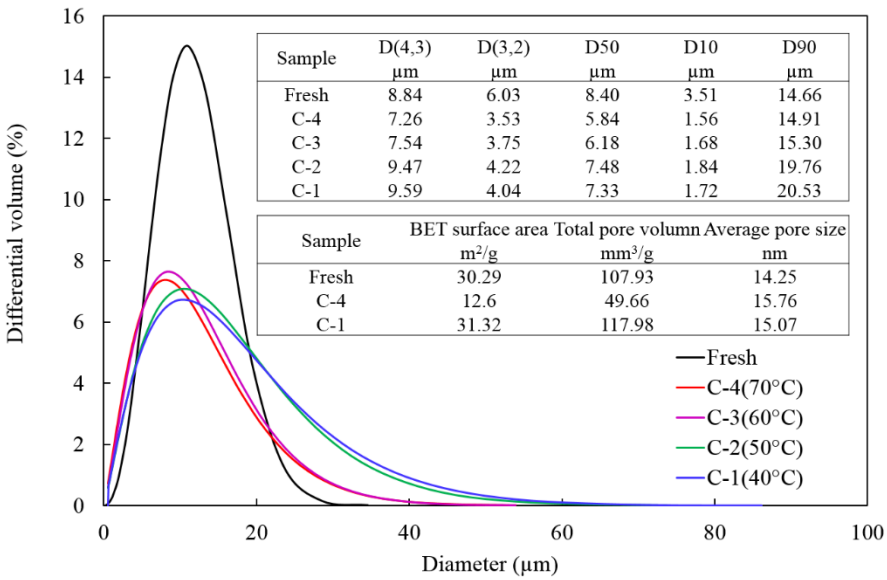

Sample	D(4,3) μm	D(3,2) μm	D50 μm	D10 μm	D90 μm
Fresh	8.84	6.03	8.40	3.51	14.66
C-4	7.26	3.53	5.84	1.56	14.91
C-3	7.54	3.75	6.18	1.68	15.30
C-2	9.47	4.22	7.48	1.84	19.76
C-1	9.59	4.04	7.33	1.72	20.53

Sample	BET surface area m^2/g	Total pore volumn mm^3/g	Average pore size nm
Fresh	30.29	107.93	14.25
C-4	12.6	49.66	15.76
C-1	31.32	117.98	15.07

Figure 4 Particle size distribution of the fresh and carbonated fly ash (stirring rate, 900 rpm; CO_2 pressure, 4 bar; temperature, 40, 50, 60 and 70 °C) fly ash

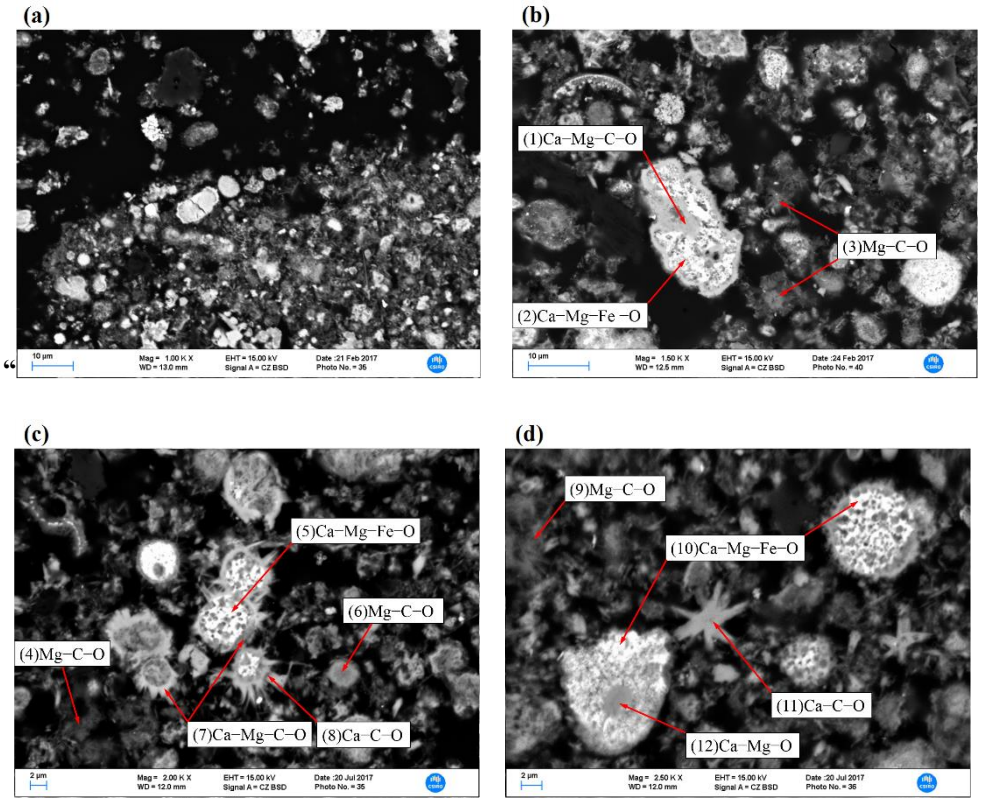

Figure 5 SEM images of (a) fresh fly ash, and (b) to (d) carbonated fly ash (temperature, 40ºC; stirring rate, 900 rpm; CO_2 pressure, 4bar)

List of tables

Table 1 Summary of physicochemical properties of fly ash

	Items	Unit	Fresh ash
Physical properties	D[4,3]	µm	8.84
	D[3,2]	µm	6.03
	D10	µm	3.51
	D50	µm	8.40
	D90	µm	14.66
	BET surface area	m^2/g	30.29
Chemical properties	SiO_2	wt%	5.8
	Al_2O_3	wt %	3.0
	Fe_2O_3	wt%	14.0
	CaO	wt%	32.4
	MgO	wt%	29.3
	TiO_2	wt%	0.7
	Na_2O	wt%	0.2
	K_2O	wt%	0.2
	P_2O_5	wt%	0.4
	MnO	wt%	0.7
	SO_3	wt%	12.8
CO_2 (Titration)		g-CO_2/g-FA	0.166
Theoretical CO_2 sequestration capacity		g-CO_2/g-FA	256.4

Table 2 The relative concentrations (wt.%) of the phases identified in the fresh and carbonated fly ash

Id.	Chemical formula	Fresh ash	Carbonated ash
Quartz	SiO_2	1.3	1.0
Augite	$(Ca,Na)(Mg,Fe,Al,Ti)(Si,Al)_2O_6$	2.2	5.3
Srebrodolskite	$Ca_2Fe_2O_5$	3.0	2.2
Gypsum	$CaSO_4 \cdot 2H_2O$	3.0	0.4
Bassanite	$CaSO_4 \cdot 0.5H_2O$	10.7	4.8
Calcite	$CaCO_3$	23.0	36.8
Aragonite	$CaCO_3$	-	2.6
Mg-calcite	$MgCO_3$	-	10.5
Brucite	$Mg(OH)_2$	4.8	-
Periclase	MgO	3.2	-
Hexahydrite	$MgSO_4 \cdot 6H_2O$	-	2.1
Pyroaurite	$Mg_6 Fe_2CO_3(OH)_{16} \cdot 4H_2O$	25.6	11.6
Amorphous	-	23.2	22.4

Table 3 Data fitting of models

No.	Equations	Mechanism	R^2
1	$kt=(1-\delta)^{-1/2}-1$	Three-halves-order kinetics	0.7779
2	$kt=(1-\delta)^{-1}-1$	Second-order kinetics	0.7929
3	$kt=1-(1-\delta)^{1/3}$	Three-dimensional advance of the reaction interface	0.7518
4	$kt=[1-(1-\delta)^{1/3}]2$	Jander; three-dimensional	0.8710
5	$kt=1-2\delta/3-(1-\delta)^{2/3}$	Crank-Ginstling-Brounshtein, mass transfer across a nonporous product layer	0.8646
6	$kt=[1-(1-\delta)^{1/2}]2$	Jander; cylindrical diffusion	0.8663
7	$kt=1/(1-\delta)^{1/3}-1$	Dickinson, Heal, transfer across the contacting area	0.7728
8	$kt=1-3(1-\delta)^{2/3}+2(1-\delta)$	Shrinking core, product layer (different form of Crank-Ginstling-Brounshtein)	0.8646
9	$kt=(1-\delta)\mathrm{Ln}(1-\delta)+\delta$	Two-dimensional diffusion	0.8612
10	$kt=(-\ln(1-\delta))^{1/3}$	Avrami-Erofeev; three-dimensional	0.5994

Table 4 Kinetic parameters of the surface coverage model at various operation conditions

No.	Operation conditions				Carbonation efficiency		Model parameters					
	Stirring rate	Temp.	P_{CO2}	Additive	Exp.	Model	k_s ($\times 10^{-6}$)	k_p ($\times 10^{2}$)	k_1 ($\times 10^{-3}$)	k_2 ($\times 10^{-2}$)	k_s*k_p ($\times 10^{-4}$)	R^2
	rpm	°C	bar	mol/L	%	%	mole/s/m^2	m^2/mol	s^{-1}	-	min^{-1}	-
1	900	40	4	-	27.7	29.0 ±0.087	1.773 ±0.018	0.929 ±0.002	4.780 ±0.042	3.447 ±0.010	1.649 ±0.018	0.9915
2	900	50	4	-	26.3	26.4 ±0.076	1.866 ±0.020	1.023 ±0.002	5.030 ±0.049	3.793 ±0.011	1.909 ±0.022	0.9894
3	900	60	4	-	24.6	24.6 ±0.037	2.356 ±0.019	1.097 ±0.002	6.350 ±0.042	4.070 ±0.006	2.586 ±0.019	0.9944
4	900	70	4	-	23.1	23.3 ±0.044	2.170 ±0.019	1.158 ±0.001	5.850 ±0.047	4.296 ±0.008	2.515 ±0.023	0.9916
5	900	40	4	-	27.1	26.7 ±0.060	1.743±0.016	1.008 ±0.003	4.700 ±0.033	3.739 ±0.008	1.757 ±0.015	0.9942
6	1050	40	4	-	27.4	26.6 ±0.043	2.311 ±0.018	1.012 ±0.003	6.230 ±0.041	3.753 ±0.006	2.339 ±0.018	0.9947
7	1200	40	4	-	27.3	27.0 ±0.071	1.714 ±0.016	0.998 ±0.002	4.620 ±0.037	3.703 ±0.010	1.711 ±0.017	0.9927
8	1350	40	4	-	27.4	26.8 ±0.050	1.910 ±0.018	1.006 ±0.002	5.150 ±0.033	3.731 ±0.007	1.920 ±0.015	0.9952
9	900	40	3	-	23.1	23.1 ±0.075	1.213 ±0.012	1.166 ±0.002	3.270 ±0.026	4.327 ±0.014	1.413 ±0.015	0.9929
10	900	40	4	-	27.1	26.7 ±0.059	1.751 ±0.015	1.009 ±0.002	4.720 ±0.033	3.741 ±0.008	1.765 ±0.015	0.9945
11	900	40	5	-	28.8	28.4 ±0.062	2.211 ±0.014	0.948 ±0.003	5.960 ±0.047	3.518 ±0.008	2.097 ±0.019	0.9927
12	900	40	6	-	30.8	31.2 ±0.067	2.511 ±0.012	0.864 ±0.002	6.770 ±0.055	3.205 ±0.007	2.170 ±0.020	0.9923
13	900	40	7	-	32.2	32.1 ±0.071	2.437 ±0.010	0.840 ±0.004	6.570 ±0.052	3.115 ±0.007	2.047 ±0.019	0.9926
14	900	40	4	0.5	33.4	31.9 ±0.053	2.819 ±0.024	0.845 ±0.002	7.600 ±0.052	3.133 ±0.005	2.381 ±0.018	0.9940
15	900	50	4	0.5	31.0	29.1 ±0.055	2.901 ±0.029	0.926 ±0.002	7.820 ±0.066	3.436 ±0.006	2.686 ±0.025	0.9907
16	900	60	4	0.5	28.0	26.8 ±0.053	2.986 ±0.029	1.007 ±0.002	8.050 ±0.078	3.735 ±0.007	3.006 ±0.032	0.9877